

Fig 1. Representative result of the cDNA macroarray of the tissue from an abdominal aortic aneurysm. (A) Control, (B) diseased tissue.

Table 1 Sequence of Primer and Probe

IL8 sense	TCTAGGACAAGAGCCAGGAAGAA
IL8 antisense	GGCCAGCTTGGAGTCATGT
IL8 TaqMan	CACCGGAAGGAACCATCTCACTGTGTGTGA
CXCR2 sense	TACATGGCTTGATCAGCAAGGA
CXCR2 antisense	GCCCTGAAGAAGAGCCAACA
CXCR2 TaqMan	TGCCAAAGACAGCAGGCCITTCCT
CCR2 sense	GCCGCTGCTCATCATGGT
CCR2 antisense	TGCCTCTTCTCTCGTTTCGA
CCR2 TaqMan	ACTCGGGAATCCTGAAAACCCGTCTTC

The sequences of the primer and probe of MCP-1 were provided by on-line TaqMan gene expression assays (Assay ID Hs 00234140_m1).

(Histochoice, Hedwin, Baltimore, MD, USA). After overnight fixation, the samples were paraffin embedded and sectioned at 4 μ m intervals. Tissue sections were deparaffinized with xylene followed by immersion in graded alcohol. They were washed 3 times for 5 min each in phosphate-buffered saline (PBS) and blocked with bovine serum albumin for 60 min. Specimens were then incubated with primary antibodies (Fuji Chemical, Tokyo, Japan) overnight at 4°C. After they were washed in PBS, specimens were incubated with biotinylated rabbit anti-mouse IgG for 60 min at room temperature. Specimens were then washed with PBS, stained with horseradish peroxidase-conjugated streptavidin, and finally incubated with substrate solution for 1–15 min. The tissue sections were also stained with hematoxylin-eosin.

Statistical Analysis

The mean and standard error of triplicate data are presented. Statistical analysis was performed by Mann-Whitney test and Wilcoxon signed-rank test using Stat View 5.0 software (Abacus Concepts, Calabasus, CA, USA) on a Macintosh computer. A p-value <0.05 was considered significant.

Results

cDNA Macroarray for AAA Tissues

A representative autoradiograph of the human cytokine expression array after hybridization with cDNA probes derived from AAA and adjacent control tissues is shown in Fig 1. Although densitometric analysis revealed significant (>5-fold) upregulation of 97 of the 375 genes, 23 genes appeared to be overexpressed by visual inspection. Under these conditions, 10 cytokine-related genes were strongly overexpressed in comparison with those in the adjacent control tissues: Activin R1A (TGF b superfamily, 13:1), Activin R1B (TGF b superfamily, 12:1), BMP RIIA (TGF b superfamily, 12:1), CXCR-5 (chemokine receptor, 12:1), CXCR-2 (chemokine receptor, 11:1), IL-8 (chemokine, 9:1), CCR-6 (chemokine receptor, 9:1), BMP RIA (TGF b superfamily, 8:1), CXCR-1 (chemokine receptor, 7:1), and CXCR-6 (chemokine receptor, 7:1). It was interesting that IL-8 and its receptor, CXCR-2, were simultaneously up-regulated, suggesting their significant role in disease development. Therefore, these 2 genes were quantitatively determined by real-time RT-PCR with TaqMan probes (Table 1). Additionally, in some patients the expressions of MCP-1 and its receptor, CCR-2, were determined by the same procedures.

In AAA, the expression of IL-8 and CXCR-2 in CAS was 0.53 ± 0.16 and 2.04 ± 0.75 , respectively and significantly greater than those in the adjacent control tissues in which the expressions were 0.11 ± 0.04 and 0.29 ± 0.10 ($p < 0.01$), respectively. Under these conditions, the expressions of MCP-1 and CCR-2 in the diseased portion were slightly upregulated at 1.51 ± 0.38 and 1.24 ± 0.10 , respectively, in comparison with those in adjacent control tissues (0.32 ± 0.08 and 0.28 ± 0.09 , respectively, $n = 4$).

In CAS, expression of IL-8 and CXCR-2 in CAS was 1.35 ± 0.25 and 2.00 ± 0.51 , respectively and significantly greater than that in the adjacent control tissues where it was 0.60 ± 0.16 and 0.58 ± 0.21 ($p < 0.05$), respectively (Fig 2). Under these conditions, there was no statistical significance

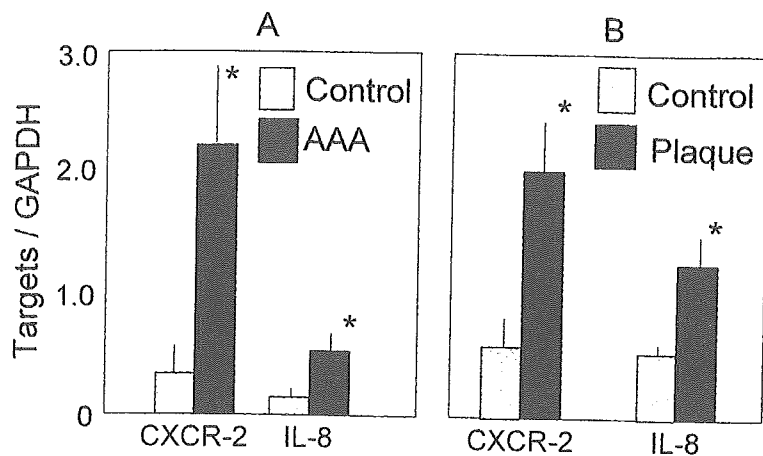


Fig 2. Expression of CXCR-2 and interleukin (IL)-8 in (A) abdominal aortic aneurysm (AAA) and (B) carotid artery stenosis (CAS).

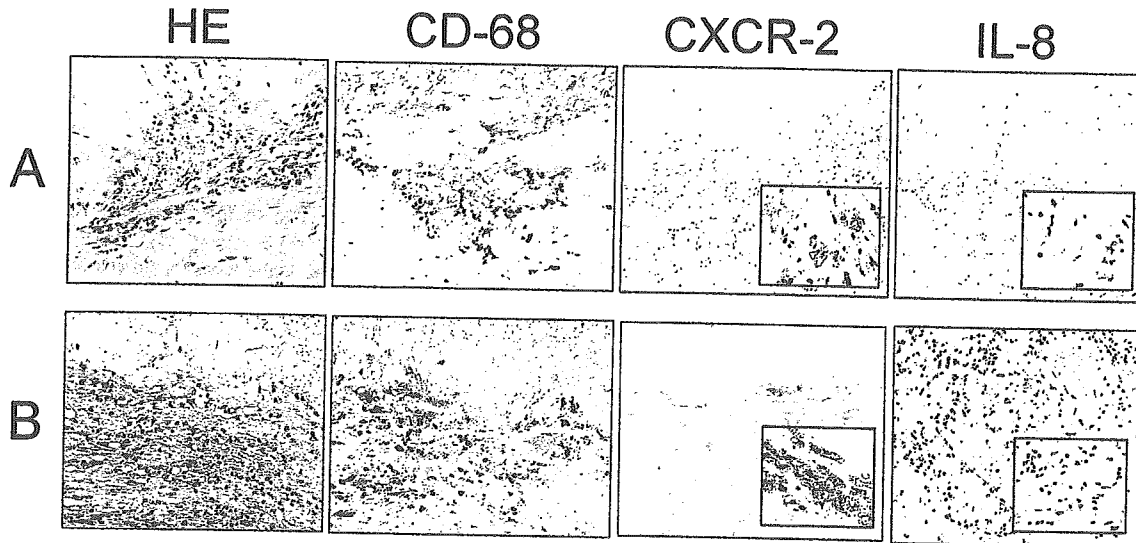


Fig 3. Immunohistochemistry of tissue samples from (A) abdominal aortic aneurysm and (B) carotid artery stenosis (Original magnification $\times 100$; Insert: $\times 400$).

in the expressions of MCP-1 and CCR-2 in diseased (0.44 ± 0.15 and 2.72 ± 1.76 , respectively) and control (0.38 ± 0.11 and 0.99 ± 0.18 , $n=13$) tissues.

Immunohistochemistry

In both AAA and CAS tissues, the control regions exhibited mild atherosclerosis in which a few CD-68 positive macrophages existed. The specimens of AAA consisted of thinned or thickened vascular tissue in which typical atheromatous plaques with infiltration of macrophages and lymphocytes were present. Plaque regions of CAS mainly consisted of a lipid-rich core and fibrous tissue in which CD-68 positive macrophages had accumulated, particularly in the shoulder regions of the atheroma. Under these conditions, IL-8 and CXCR-2 were mainly expressed in the macrophages, which were identified as CD68-positive cells in each tissue (Fig 3).

Discussion

In the present study, we used cDNA macroarray to try and determine the possible cytokine-related mediators that could contribute to the development of atherosclerosis,

and we then quantitatively measured the expression of their mRNA using real-time RT-PCR. The inflammatory chemokine IL-8 and its receptor, CXCR-2, were demonstrated to be simultaneously upregulated in the diseased portions, suggesting their key role in the development of dilated and occlusive atherosclerotic diseases.

Determination Procedures for mRNA

The recent development of microchip- or membrane-based cDNA arrays has enabled examination of the simultaneous expression of multiple gene products of known identity, facilitating the identification of altered patterns of gene expression in a given tissue? Because this approach has the potential to reveal novel pathophysiologic insights, we first used it to characterize the simultaneous expression of approximately 375 gene products in human AAA, in which enough mRNA was collected to synthesize the cDNA, and to compare the expression profile of AAA with adjacent control tissues. We found that the expression of IL-8 (9-fold) and its receptor, CXCR-2 (11-fold) were simultaneously upregulated in the diseased portion.

However, it is necessary to reemphasize that the cDNA array is most valuable for detecting novel, unanticipated

alterations in gene expression, and that the strength of this method currently resides in its capacity to characterize patterns of gene expression rather than to quantify the expression of individual gene products. Thus, we performed quantitative analysis of gene expression with real-time RT-PCR, the accuracy of which to determine gene expression in human tissue has already been demonstrated elsewhere²

Role of Inflammatory Chemokines in Dilated and Occlusive Atherosclerotic Diseases

IL-8, a C-X-C chemokine which was upregulated in both AAA and CAS, is produced by various types of cells on stimulation with inflammatory stimuli¹⁰⁻¹³ Low density lipoprotein (LDL)-deficient mice, irradiated and reconstituted with macrophages deficient in the murine IL-8 receptor homologue of human CXCR-2, show diminished macrophage recruitment to the lesion, suggesting a potential role for IL-8 in monocyte trafficking *in vivo*.¹⁴ Moreover, IL-8 may contribute to the development of atherosclerosis by stimulating angiogenesis.¹⁵ It exerts a variety of effects on leukocytes, particularly neutrophils,¹⁶ and plays a critical role in the mobilization of stem cells through its induction of MMP-9.¹⁷ In terms of MMP synthesis in dilated and occlusive atherosclerotic diseases, we previously reported significant upregulation of the expression of MMP-1 and -3 in AAA tissues, and MMP-1, -3 and -9 in CAS tissues.^{2,3} MMP-9 is also upregulated in the infarct-related human coronary artery.^{18,19} Therefore, upregulation of IL-8 might be related to overexpression of these MMPs in human atherosclerotic tissues.

IL-8 is also known to inhibit the production of the tissue inhibitor of matrix metalloproteinases (TIMPs), which are potent antagonists of MMPs in vessel tissue.²⁰ Our previous data indicate disproportional expression of MMPs/TIMPs in AAA as well as CAS.^{2,3} Therefore, in the clinical setting upregulation of IL-8 could be related to this disproportional TIMPs expression in both AAA and CAS, thus enhancing the development of dilated or occlusive manifestation of atherosclerosis probably through the activation of proteinase activity. It has been suggested that the chemokine receptor CXCR-2 enhances monocyte recruitment and disease progression.²¹ Indeed, the lack of CXCR-2 expression in bone marrow cells has been shown to be responsible for an almost 50% reduction in lesion development.²²

There was no statistical significance in the expression of MCP-1 and CCR-2 in AAA and CAS tissues, which may be partly explained by the relatively high gene expression in the adjacent control tissues that already had minimal atherosclerotic changes. One might speculate that the MCP-1 and CCR-2 system, which is upregulated in the early stage of atherosclerosis, could be relatively downregulated in the established stage, such as the significant dilated and/or stenotic lesions studied by us. This might result in an altered balance in the expression of the contributing and suppression genes, which leads to the severity of the disease process.^{1,4}

Clinical Implications and Study Limitations

Although the precise relationship between the inflammatory process of atherosclerosis and development of AAA and/or CAS, particularly in the established stage of the diseases, remains unclear, their frequent association and shared risk factors suggest common pathophysiologic mechanisms. This assertion is supported by the observation that both AAA and CAS exhibited increased expression of

CXCR-2 as well as IL-8, both of which are thought to be important in inflammatory process of atherosclerosis, although we could not correlate the extent of disease severity with the levels of gene expression because of similar aneurysmal (>40 mm in diameter) and stenotic (>90%) lesions in the present cohort.

From the therapeutic point of view, it is interesting to note that the established anti-inflammatory pathways of HMG-CoA reductase inhibitors include the diminished expression of cytokines, such as IL-6 and IL-8, in cells implicated in atherogenesis or in human plasma.^{23,24} In addition, oxidized LDL-cholesterol enhances the upregulation of the expression of CXCR-2 in monocytes, contributing to disease progression associated with dilation or occlusion.²⁵ Indeed, atorvastatin therapy, which suppresses the development of atherosclerosis as well as reduces the incidence of major adverse cardiac events,^{26,27} could decrease the spontaneous release of IL-8 in mononuclear cells of patients with coronary artery disease.²⁸ Also, the effects of angiotensin-receptor inhibitors on suppression of atherosclerosis could be derived from inhibition of the overexpression of chemokines, such as IL-8, associated with reduction of macrophage accumulation in the lesion.²⁹ Although it would be indeed intriguing to examine whether the expressions of IL-8 and CXCR-2 in AAA and CAS could be affected by these "anti-inflammatory" drugs in the present cohort, we could not correlate gene expression level to treatment because of the variety of drugs and their doses. A prospective study of intensive use of HMG-CoA reductase inhibitors and/or angiotensin-receptor inhibitors for AAA and CAS patients may demonstrate the effectiveness of these agents on the expression of IL-8 and CXCR-2 and whether this is protective or not in the established stage of dilated and/or stenotic lesions.

One of the most important limitations in the present study is that we used the adjacent tissues, which were already involved in the disease, as the control. Therefore, the present study was not done with truly normal tissue. However, both control tissues did not show any dilated or occlusive lesions and might be considered to be in the "preaneurymal" or "preocclusive" state of the disease.

Even under these conditions, upregulation of IL-8 and associated CXCR-2 may have a crucial role in the development of manifested atherosclerotic disease.

Conclusions

We used a membrane-based cDNA macroarray and real-time RT-PCR to characterize the cytokine-related gene expression in AAA and CAS. Although the functional significance of the individual gene products that were altered in AAA and CAS will require further investigation, this study demonstrates the potential of cDNA expression array and real-time RT-PCR in elucidating the molecular mechanisms responsible for the development of AAA and CAS.

Acknowledgments

We appreciate the invaluable comments from Professor Kouji Matsushima, MD, Division of Molecular and Preventive Medicine, University of Tokyo, Tokyo, Japan. This work is dedicated to Dr Michihiko Tada, Honorary Professor of Medicine, Osaka University School of Medicine who has always encouraged us to perform research works.

This work was supported by the grants from the Minister of Health, Welfare and Labor of Japan (to M.Y.), from the Japan Cardiovascular Research Foundation (to A.S.) and by the Grant for Clinical Vascular Function from Kimura Memorial Cardiovascular Research Foundation (to T.H.).

References

- Libby P. Inflammation in atherosclerosis. *Nature* 2002; **420**: 868–874.
- Higashikata T, Yamagishi M, Sasaki H, Minatoya K, Ogino H, Ishibashi-Ueda H, et al. Application of real-time RT-PCR to quantifying gene expression of matrix metalloproteinases and tissue inhibitors of metalloproteinases in human abdominal aortic aneurysm. *Atherosclerosis* 2004; **177**: 353–360.
- Higashikata T, Yamagishi M, Higashi T, Nagata I, Iihara K, Miyamoto S, et al. Altered expression balance of matrix metalloproteinases and their inhibitors in human carotid plaque disruption: Results of quantitative tissue analysis using real-time RT-PCR method. *Atherosclerosis* 2005 July 20; [Epub ahead of print].
- Boring L, Gosling J, Cleary M. Decreased lesion formation in CCR2^{-/-} mice reveals a role for chemokines in the initiation of atherosclerosis. *Nature* 1998; **394**: 894–897.
- Ito T, Ikeda U. Inflammatory cytokines and cardiovascular disease. *Curr Drug Targets Inflamm Allergy* 2003; **2**: 257–265.
- Kusano KF, Nakamura K, Kusano H, Nishii N, Banba K, Ikeda T, et al. Significance of the level of monocyte chemoattractant protein-1 in human atherosclerosis. *Circ J* 2004; **68**: 671–676.
- Koch AE, Kunkel SL, Pearce WH, Shah MR, Parikh D, Evanoff HL, et al. Enhanced production of the chemotactic cytokines interleukin-8 and monocyte chemoattractant protein-1 in human abdominal aortic aneurysms. *Am J Pathol* 1993; **142**: 1423–1431.
- Yamagishi M, Higashikata T, Higashi T, Nagata I, Ishibashi-Ueda H, Tomoike H, et al. Sustained upregulation of chemokine and its receptor genes associated with matrix metalloproteinase overexpression in human carotid plaque rupture: Results from a quantitative study with real-time RT-PCR method (abstract). *J Am Coll Cardiol* 2004; **43**(Suppl A): 497A.
- Faber BC, Cleutjens KB, Niessen RL, Aarts PL, Boon W, Greenberg AS, et al. Identification of genes potentially involved in rupture of human atherosclerotic plaques. *Circ Res* 2001; **89**: 547–554.
- Matsushima K, Oppenheim JJ. Interleukin 8 and MCAF: Novel inflammatory cytokines inducible by IL-1 and TNF. *Cytokine* 1989; **1**: 2–13.
- Boisvert WA, Curtiss LK, Terkeltaub RA. Interleukin-8 and its receptor CXCR2 in atherosclerosis. *Immunol Res* 2000; **21**: 129–137.
- Yound JL, Libby P, Schonbeck U. Cytokines in the pathogenesis of atherosclerosis. *Thromb Haemost* 2002; **88**: 554–567.
- Hansson GK, Libby P, Schonbeck U, Yan ZQ. Innate and adaptive immunity in the pathogenesis of atherosclerosis. *Circ Res* 2002; **91**: 281–291.
- Boisvert WA, Santiago R, Curtiss LK. A leukocyte homologue of the IL-8 receptor CXCR-2 mediates the accumulation of macrophages in atherosclerotic lesions of LDL receptor-deficient mice. *J Clin Invest* 1998; **101**: 353–363.
- Simonini A, Moscucci M, Muller DW, Bates ER, Pagani FD, Burdick MD. IL-8 is an angiogenic factor in human coronary atherectomy tissue. *Circulation* 2000; **101**: 1519–1526.
- Chakrabarti S, Patel KD. Regulation of matrix metalloproteinase-9 release from IL-8-stimulated human neutrophils. *J Leukoc Biol* 2005; **78**: 279–288.
- Pruijt JF, Verzaal P, van Os R, de Kruijff EJ, van Schie ML, Mantovani A, et al. Neutrophils are indispensable for hematopoietic stem cell mobilization induced by interleukin-8 in mice. *Proc Natl Acad Sci USA* 2002; **99**: 6228–6233.
- Funayama H, Ishikawa SE, Kubo N, Katayama T, Yasu T, Saito M, et al. Increases in interleukin-6 and matrix metalloproteinase-9 in the infarct-related coronary artery of acute myocardial infarction. *Circ J* 2004; **68**: 451–454.
- Higo S, Uematsu M, Yamagishi M, Ishibashi-Ueda H, Awata M, Morozumi T, et al. Elevation of plasma matrix metalloproteinase-9 in the culprit coronary artery in patients with acute myocardial infarction: Clinical evidence from distal protection. *Circ J* 2005; **69**: 1180–1185.
- Moreau M, Brocheriou I, Petit L, Ninio E, Chapman MJ, Rouis M. Interleukin-8 mediates downregulation of tissue inhibitor of metalloproteinase-1 expression in cholesterol-loaded human macrophages: Relevance to stability of atherosclerotic plaque. *Circulation* 1999; **99**: 420–426.
- Holm T, Damas JK, Holven K, Nordoy I, Brosstad FR, Ueland T, et al. CXC-chemokines in coronary artery disease: Possible pathogenic role of interactions between oxidized low-density lipoprotein, platelets and peripheral blood mononuclear cell. *J Thromb Haemost* 2003; **1**: 257–262.
- Huo Y, Weber C, Forlow SB, Sperandio M, Thatte J, Mack M, et al. The chemokine KC, but not monocyte chemoattractant protein-1, triggers monocyte arrest on early atherosclerotic endothelium. *J Clin Invest* 2001; **108**: 1307–1314.
- Takata M, Urakaze M, Temaru R, Yamazaki K, Nakamura N, Nobata Y. Pravastatin suppresses the interleukin-8 production induced by thrombin in human aortic endothelial cells cultured with high glucose by inhibiting the p44/42 mitogen activated protein kinase. *Br J Pharmacol* 2001; **134**: 753–762.
- Ito T, Ikeda U, Yamamoto K, Shimada K. Regulation of interleukin-8 expression by HMG-CoA reductase inhibitors in human vascular smooth muscle cells. *Atherosclerosis* 2002; **165**: 51–55.
- Lei ZB, Zhang Z, Jing Q, Qin YW, Pei G, Cao BZ, et al. OxLDL upregulates CXCR2 expression in monocytes via scavenger receptors and activation of p38 mitogen-activated protein kinase. *Cardiovasc Res* 2002; **53**: 524–532.
- Nissen SE, Tuzcu EM, Schoenhagen P, Brown BG, Ganz P, Vogel RA, et al. Effect of intensive compared with moderate lipid-lowering therapy on progression of coronary atherosclerosis: A randomized controlled trial. *JAMA* 2004; **291**: 1071–1080.
- Cannon CP, Braunwald E, McCabe CH, Rader DJ, Rouleau JL, Belder R, et al. Intensive versus moderate lipid lowering with statins after acute coronary syndromes. *N Engl J Med* 2004; **350**: 1495–1504.
- Wahre T, Damas JK, Gullestad L, Holm AM, Pedersen TR, Arnesen KE, et al. Hydromethylglutaryl coenzyme A reductase inhibitors down-regulate chemokines and chemokine receptors in patients with coronary artery disease. *J Am Coll Cardiol* 2003; **41**: 1460–1467.
- Dol F, Martin G, Staels B, Mares AM, Cazaubon C, Nisato D, et al. Angiotensin AT1 receptor antagonist Irbesartan decreases lesion size, chemokine expression, and macrophage accumulation in apolipoprotein E-deficient mice. *J Cardiovasc Pharmacol* 2001; **38**: 395–405.

Culturing Human Mesenchymal Stem Cells on Bioceramics for Hard Tissue Regeneration (Validation of *In Vitro* Bone Matrix Formed on Ceramics for Clinical Application)

Hajime Ohgushi^{1,a}, Shigeyuki Kitamura², Noriko Kotobuki¹, Motohiro Hirose¹
Hiroko Machida¹, Akira Oshima¹, Yasuhito Tanaka³ and Yoshinori Takakura³

¹Tissue Engineering Research Group, Research Institute for Cell Engineering (RICE), National Institute of Advanced Industrial Science and Technology (AIST), 3-11-46 Nakouji, Amagasaki City, Hyogo 661-0974, Japan

²Department of Orthopaedic Surgery, Nippon Medical School, 1-1-5 Sendagi, Bunkyo-ku, Tokyo 113-8603, Japan

³Department of Orthopaedic Surgery, Nara Medical University, Kashihara, Nara 634-8522, Japan

^ahajime-ohgushi@aist.go.jp

Keywords: Alumina Ceramics, Bone Marrow, Tissue Culture, Tissue Engineering

Abstract

Alumina ceramics have excellent mechanical and biocompatible properties, but are bioinert and hence have no bone-bonding properties. We took a tissue engineering approach in an attempt to modify the ceramic surface and so provide an osteogenic/osteoconductive milieu. We used fresh human bone marrow cells obtained from the iliac crest by needle aspiration for culture expansion of mesenchymal stem cells (MSC) followed by *in vitro* osteogenic differentiation on both tissue culture polystyrene (TCPS) and alumina ceramics. We have succeeded in expanding the number of MSC from all 35 cases and compared the differentiation capability of selected MSC on alumina ceramics to that on TCPS. The cells on both substrata showed extensive alkaline phosphatase staining and mineralization as evidenced by calcein uptake. Biochemical analyses revealed high levels of alkaline phosphatase activity, osteocalcin expression, and calcium content. These data indicate that an alumina ceramic surface can support a differentiation cascade of MSC resulting in osteoblastic phenotype expression of the cells. Based on these results, we have performed clinical applications of tissue engineered total joint replacements for osteoarthritic patients.

Introduction

Mesenchymal stem cells (MSC) are multipotent cells that can be isolated from adult bone marrow and can be induced *in vitro* and *in vivo* to differentiate into a variety of mesenchymal tissues including bone, cartilage, tendon, fat, and bone marrow stroma [1]. We have already used culture expanded MSC from patients for hard tissue repair. Our approach utilizes the MSC followed by osteogenic differentiation on various bioceramics; the differentiation was accompanied by bone matrix formation on the bioceramic surface [2,3]. This matrix formation is especially important for the use of bioinert ceramics such as alumina ceramics because the bone matrix consists of biological apatite (low crystallized carbonated apatite) [4]. Thus, matrix formation on a bioinert ceramic surface can convert the ceramic into bioactive ceramic. However, in considering clinical applications, the capability of bone matrix formation of human MSC and the capability of bioinert ceramics should be determined [5]. In this paper, we focus on proliferation associated with bone matrix formation of human MSC on both tissue culture polystyrene (TCPS) and alumina ceramic surfaces. The MSC were derived from human aspirated bone marrow from 35 human donors.

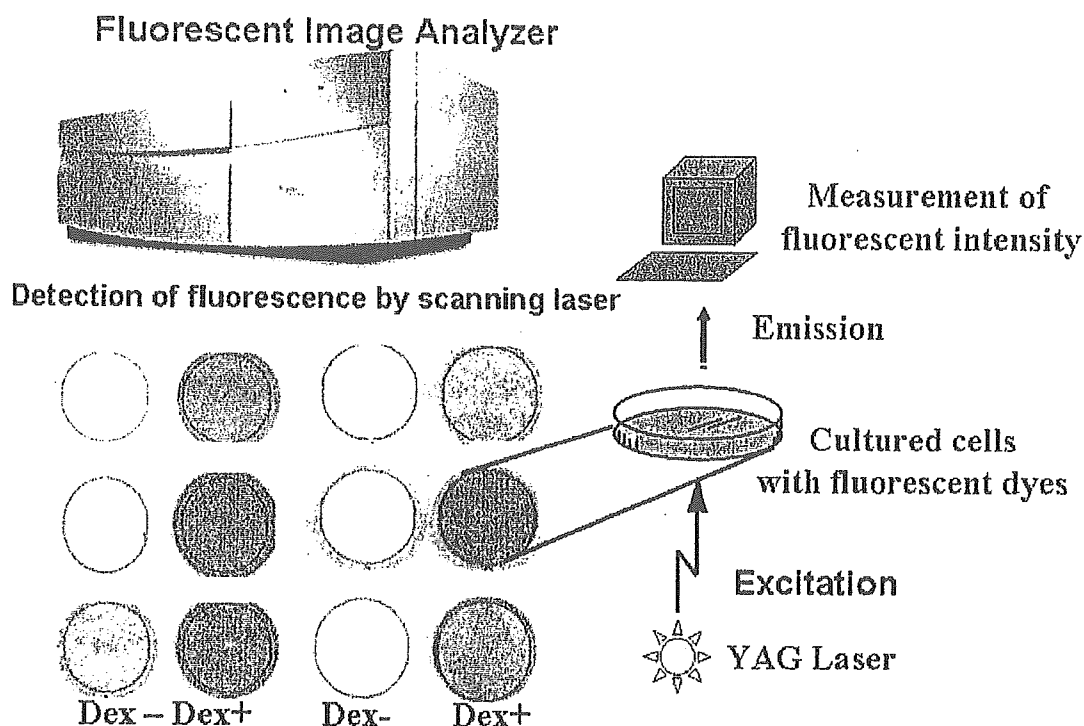


Fig. 1 Fluorescence intensity measurement of fluorescent dyes incorporated into extracellular bone matrices produced by human mesenchymal stem cells (MSC). The figure at lower left shows the fluorescent images of MSC cultured in the presence (Dex +) or absence (Dex -) of dexamethasone from 6 independent cases.

Materials and Methods

Materials: Alumina ceramic disks (30 mm diameter, 1.5 mm thick) were kindly provided by Kyocera Co. (Kyoto, Japan). The disks, which consisted of 99.5% pure polycrystalline-alumina, were produced by sintering pressed alumina powder at 1500°C. To enable the use of an optical microscope to observe the cultured cells on the ceramic, we also used transparent single-crystal alumina disks that were manufactured using the Czochralski crystal growth technique [5].

Marrow cell preparation and culture: Human bone marrow cells removed from the iliac crest of 35 donors by needle aspiration after obtaining informed consent were used for the primary culture. The medium consisted of Eagle's minimum essential medium alpha (alpha-MEM). The culture medium was renewed three times a week and adherent cells of mesenchymal types proliferated [6]. After trypsinization, the cells were seeded into control tissue culture polystyrene (TCPS) dishes or onto alumina disks [5,7]. The samples were then subcultured for two weeks with medium supplemented with glycerophosphate, ascorbic acid, and with or without dexamethasone (Dex) [8,9]. For the assay of bone matrix formation, 1 µg/mL calcein was added [10]. Fluorescence of the incorporated calcein was visualized and quantified by using an image analyzer (Typhoon 8600, Molecular Dynamics Inc., CA, USA) (526 nm short-pass filter) and was observed by using a confocal laser microscope (LSM510, Carl Zeiss Co., Ltd., Germany).

Biochemical assay: After the quantification of the calcein uptake, the cells were washed twice with PBS (-) after which 1 mL of 20% formic acid was added. The calcium content was measured using an inductively coupled plasma atomic emission spectrometer (SPS7800 plasma spectrometer, Seiko Instruments Inc., Chiba, Japan). DNA, alkaline phosphatase, and osteocalcin were also measured as described previously [4,5].



Fig. 2 Phase contrast microscopy of human mesenchymal stem cells (MSC) cultured on alumina ceramics. The culture was done in the presence of dexamethasone. The black areas at Day 14 indicate mineral deposition after 14 days of culture.

Results and conclusion

Fresh human marrow cells were cultured on tissue culture polystyrene (TCPS) plates and showed extensive proliferation of mesenchymal stem cells (MSC) from all donors (16 – 85 years old). The subculture of the MSC on TCPS in the presence of Dex (Dex +) produced a bone matrix formation as evidenced by the fluorescent (calcein) uptake, as shown in Fig. 1. We also performed quantitative and qualitative assays of the osteogenic potential of MSC on both TCPS and alumina ceramic surfaces for selected cases. During the two-week subculture period, proliferation and differentiation of the MSC on the alumina disks as well as the control TCPS dishes were compared by phase contrast microscopy. The Dex-treated cells showed good cell adhesion accompanied by cell spreading not only in the TCPS dishes but also on the alumina disks (Fig. 2). Subsequently, the cells cultured on both substrates showed a similar pattern of proliferation, and reached confluence at day 8. At day 14 of the subculture, the Dex-treated cells cultured on both the alumina disks and in the TCPS dishes formed nodular aggregates indicating mineralization (black areas in Fig. 2, Day 14). In contrast, the cells not treated with Dex did not exhibit these aggregates (data not shown). Thus, cell attachment to substrates, proliferation, and the mineralization of MSC occurred in much the same way on the alumina surface as well as on the TCPS dish surface.

After 14 days of subculture, biochemical analyses were done for the cell layers on the alumina disks and control TCPS dishes. For every case of MSC, the DNA content on the alumina disks was similar to that in the TCPS dishes regardless of the Dex treatment. ALP activity, which is recognized as an osteoblastic marker, was significantly higher on all substrates in the Dex-treated cells than that in the untreated cells. In all cases, the bone-specific osteocalcin and calcium contents on both the alumina disks and TCPS dishes were also significantly higher in the Dex-treated cells than in the cells not treated with Dex.

The data indicate that a high osteogenic potential could be observed on both TCPS and alumina ceramics. In conclusion, our results confirm the capability of osteogenic differentiation of human MSC cultured on various culture substrata including alumina ceramic. Importantly, the cells were derived from bone marrow obtained with minimum invasion using needle aspiration. We have already cultured a patient's MSC on alumina ceramics for a complete ankle and used this for total joint replacement surgery (Fig. 3). Current tissue-engineered approaches using bioceramics have clinical significance for reconstruction in the field of hard tissue regeneration.

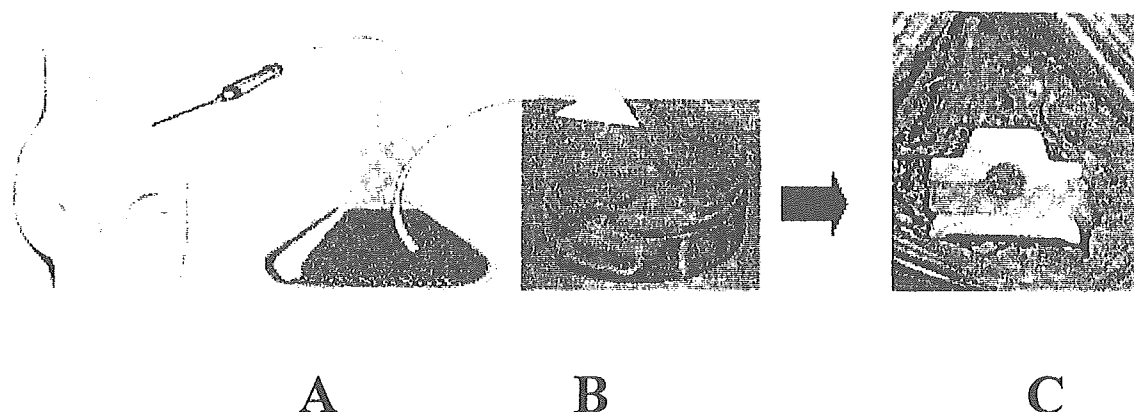


Fig. 3 Approach for fabricating a tissue engineered ankle prosthesis: A) Proliferation of mesenchymal cells (MSC) from the patient's bone marrow by culture; B) Osteogenic differentiation of the MSC resulting in the appearance of bone-forming osteoblasts together with the formation of bone matrix on the ceramic prosthesis; and C) Implantation of the prosthesis in the same patient.

Acknowledgments

This work was undertaken by the Three-Dimensional Tissue Module Project, METI (A Millennium Project); Grant-in-Aid for Scientific Research Japan supported this work. We wish to express our gratitude to Kyocera Co., Ltd. (Kyoto, Japan) for supplying the alumina ceramic disks.

References

1. Caplan AI, *Clin Plast Surg*. 1994 Jul;21(3):429-35
2. Ohgushi H, Caplan AI. *J Biomed Mat Res* 1999;48:913-27
3. Ohgushi H, Miyake J, Tateishi T. *Novartis Found Symp*. 2003;249:118-27
4. Ohgushi H, Dohi Y, Katuda T, Tamai S, Tabata S, Suwa Y. *J Biomed Mat Res* 1996;32:333-40.
5. Kitamura S, Ohgushi H, Hirose M, Funaoka H, Takakura Y, Ito H. *Artif Organs*. 2004 Jan;28(1):72-82
6. Kotobuki N, Hirose M, Takakura Y, Ohgushi H. *Artif Organs* 2004;28:33-39.
7. Ohgushi H, Dohi Y, Yoshikawa T, Tamai S, Tabata S, Okunaga K, Shibuya T. *J Biomed Mat Res* 1996;32:341-8
8. Maniopoulos C, Sodek J, Melcher AH. *Cell Tissue Res* 1988;254:317-30.
9. Jaiswal N, Haynesworth SE, Caplan AI, Bruder SP. *J Cell Biochem* 1997;64:295-31
10. Uchimura E, Machida H, Kotobuki N, Kihara T, Kitamura S, Ikeuchi M, Hirose M, Miyake J, Ohgushi H. *Calcif Tissue Int* 2003 73(6):575-83

Chondrocyte LALP? → hydrogel
Chondrocyte
BG against cartilage biology

Development of Controlled Heterogeneity on a Polymer-Ceramic Hydrogel Scaffold for Osteochondral Repair

H.H. Lu^a, J. Jiang, A. Tang, C.T. Hung and X.E. Guo

Department of Biomedical Engineering, 351 Engineering Terrace, New York, NY 10027, USA
^ahi2052@columbia.edu

Keywords: Chondrocytes, Co-Culture, Composites, Interface Tissue Engineering, Multi-Phased Scaffold, Osteoblasts, Osteochondral Repair

Hydrogel - (Hydrogel)

Abstract. Due to its intrinsically poor repair potential, injuries to articular cartilage do not heal and clinical intervention is required. Osteochondral grafts may improve healing while promoting integration with host tissue. We report here the development of an osteochondral graft based on a hybrid of a hydrogel and a polymer-bioactive glass composite (PLAGA-BG) microsphere scaffold. This novel osteochondral construct consists of three regions: gel-only, gel/composite interface, and a composite-only-region. The three phases differ in calcium phosphate (Ca-P) or BG content. The objective of the current study is to investigate the effects of scaffold composition on chondrocyte response, and to evaluate the effects of co-culture on osteoblasts and chondrocyte growth and differentiation on the hybrid scaffold. The PLAGA-BG microsphere scaffold supported the growth of chondrocytes and initial results indicate that in the presence of BG, chondrocyte-mediated mineralization may be stimulated. Co-culture of osteoblasts and chondrocytes on the multi-phased scaffold with varied Ca-P content facilitated the formation of multiple matrix zones: a GAG-rich chondrocyte region, an interfacial matrix rich in GAG+collagen, and a mineralized collagen matrix with osteoblasts. In summary, chondrocyte response has been optimized as a function of scaffold composition and the novel osteochondral graft has the potential to support the simultaneous formation of multiple types of tissue *in vitro*.

INTRODUCTION

Injuries to articular cartilage do not heal and limited success has been achieved with biological grafts and cell-based therapies. It has been observed that cartilage injuries extended to subchondral bone undergo only partial repair[1]. Therefore, it is likely that an osteochondral graft can improve healing while promoting integration with host tissue. We believe that the re-establishment of a continuous interface on the osteochondral graft is critical to long term success of the composite implant system intended for cartilage repair. The native osteochondral interface bridges bone and cartilage, and is comprised of a mineralization front or tidemark which demarcates the mineralized cartilage and subchondral bone from the non-mineralized deep zone cartilage. The primary function of the interface is to redistribute the complex loads and strains between bone and cartilage, while acting as a conduit of nutrients and cells for the otherwise poorly vascularized soft tissue.

In the past decade, tissue engineering has emerged as an alternative approach to implant design and tissue regeneration. Design methodologies derived from current tissue engineering efforts can be readily applied to regenerate the osteochondral interface. This paper describes the development of an *in vitro* graft system for the regeneration of the osteochondral interface. The native osteochondral interface spans from nonmineralized cartilage to bone, thus one of the biomimetic design parameters for the multiphased osteochondral graft is the calcium phosphate (Ca-P) content of the scaffold. The components of this graft system include 1) a hybrid scaffold of hydrogel and polymer-ceramic composite (PLAGA-BG), 2) novel co-culture of osteoblasts and chondrocytes, and 3) a multi-phased scaffold design comprised of three regions intended for the formation of three distinct tissue types: cartilage, interface, and bone. In the current design, Ca-P content will be related to the percent of BG in the PLAGA-BG composite. From a material selection standpoint, one phase of the hydrogel-polymer ceramic scaffold is based on a thermal setting hydrogel which has been shown to develop a functional cartilage-like matrix *in*

Technical note

Tissue engineered ceramic artificial joint—ex vivo osteogenic differentiation of patient mesenchymal cells on total ankle joints for treatment of osteoarthritis

Hajime Ohgushi^{a,*}, Noriko Kotobuki^a, Hiroyuki Funaoka^b, Hiroko Machida^a,
Motohiro Hirose^a, Yasuhito Tanaka^c, Yoshinori Takakura^c

^aResearch Institute for Cell Engineering (RICE), National Institute of Advanced Industrial Science and Technology (AIST),
Amagasaki City, Hyogo 661-0974, Japan

^bDepartment of Laboratory Products, Dainippon Pharmaceutical Co., Suita City, Osaka 564-0053, Japan

^cDepartment of Orthopedics, Nara Medical University, Kashihara City, Nara 634-8522, Japan

Received 25 October 2004; accepted 24 November 2004

Available online 8 January 2005

Abstract

Total joint arthroplasty is the common treatment of severe cases of osteoarthritis. However, complications involving failure of the bone–prosthesis interface are significant, especially in ankle arthroplasty. To prevent this complication, we attempted a tissue engineering approach using the mesenchymal cells of the patient. We collected a small amount of fresh bone marrow cells from the patient's iliac crest and expanded the number of mesenchymal cells. We then applied the mesenchymal cells to a ceramic ankle prosthesis and cultured them to form an osteoblasts/bone matrix on the prosthesis. We used tissue engineered prostheses on three patients suffering from ankle arthritis and followed their progress for at least 2 years. Follow-up X-ray examinations revealed early radiodense appearance (bone formation) around the cell-seeded areas of the prostheses about 2 months after the operation after which a stable host bone–prosthesis interface was established. All patients showed high clinical scores after the operation and did not exhibit inflammatory reactions. These preliminary results indicate that the tissue engineering approach using autologous cultured marrow mesenchymal cells might prevent aseptic loosening of the total ankle arthroplasty.

© 2004 Elsevier Ltd. All rights reserved.

Keywords: Arthroplasty; Arthritis; Alumina ceramics; Mesenchymal cells; Osteogenesis

1. Introduction

Osteoarthritis is one of the most common types of arthritis. It is characterized by the breakdown of the joint's cartilage. Cartilage breakdown causes bones to rub against each other, resulting in complaints of pain and loss of movement. Total joint arthroplasty using a synthetic prosthesis is the most common treatment in advanced stages of arthritis. Total joint arthroplasty means the bone surfaces within the joint are surgically

removed and replaced with synthetic materials, usually a prosthesis made of durable, wear-resistant polyethylene and metal/ceramic. Over the past two decades, total joint arthroplasty has proven to be an effective means for treating severe arthritis. However, the failure rate of total ankle arthroplasty exceeds those of total hip and knee arthroplasties. Consequently, some authors have concluded that ankle arthroplasty is not indicated for the treatment of painful arthritis and that arthrodesis should be considered [1,2]. Thus, development of successful ankle arthroplasty is the challenge confronting damaged ankle joints.

The principal cause of failure of ankle arthroplasty can be ascribed to anatomic considerations (the ankle is

*Corresponding author. Tel.: +81 6 6494 7806;

fax: +81 6 6494 7861.

E-mail address: hajime-ohgushi@aist.go.jp (H. Ohgushi).

too small to accommodate the stress transfers of the prosthesis) [3]. The excess stress tends to lead to an aseptic loosening around the ankle prosthesis within the bone. In this paper, we tried to establish a novel method to solve the problem of loosening by using a tissue engineering approach. The approach utilized marrow cells, which contain mesenchymal cells having osteogenic functions [4–9], and consists of three steps: (1) Proliferation of mesenchymal cells from patient bone marrow by culture; (2) Osteogenic differentiation of the culture-expanded cells resulting in the appearance of bone-forming osteoblasts together with bone matrix formation on the ceramic ankle prosthesis; and (3) Implantation of the prosthesis in the patient (total ankle arthroplasty).

2. Materials and methods

2.1. Patients

The study included three osteoarthritic patients (Table 1). We obtained full consent from all patients in accordance with local ethics committees at both the National Institute of Advanced Industrial Science and Technology (AIST) and Nara Medical University. We diagnosed all patients as suffering from osteoarthritis of the ankle joint. The patients complained of severe pain while walking, but did not exhibit any other systemic diseases. Marrow cell harvesting and surgery were performed at the Department of Orthopedics, Nara Medical University Hospital, and the harvested cells were cultured at the Cell Processing Center (CPC) of the Research Institute for Cell Engineering. CPC consists of three clean rooms (class 1000); the cells from each patient were exclusively cultured in one CO₂ incubator according to the guidelines of the Japanese Ministry of Health, Welfare and Labor.

2.2. Culture methods

We aspirated 3 ml of fresh marrow cells from the anterior iliac crest of the patients and placed the cells in a tube containing 3 ml of heparinized phosphate buffered saline (PBS). The tube was centrifuged at 140 × g for 10 min and the supernatant of plasma with the fat layer was discarded. The residue (buffy coat and red blood cells) was equally divided and put into two T-75 flask (Coster Co., Cambridge, MA) with 15 ml of Eagle minimum essential medium (MEM) containing 15% of the patient's own serum and antibiotics, then cultured in a humidified atmosphere of 95% air with 5% CO₂ at 37 °C. After 2 days of culture, non-adherent cells were removed and 13 ml of the culture medium was added. The following medium change was done at 3 times per week. The adherent cells grew and nearly

Table 1
Proliferation/osteogenic activity of mesenchymal cells from 3 ml of patients bone marrow

Age	Sex	Follow up period (months)	Cell number after primary culture ^a	Cell number after culturing first passaged (p1) cells ^b	DNA content after culturing second passaged (p2) cells (µg/well) ^c	ALP activity after culturing p2 cells (µmol substrate released /30 min/well) ^d		Clinical score ^e					
						Dex -	Dex +	Before	3M	6M	12 M	24M	
71 yr (Case 1)	F	30	19 million/10d	53 million/6d	14.7 ± 4.45	22.2 ± 3.30**	0.07 ± 0.03	0.80 ± 0.36*	14	87	97	97	97
67 yr (Case 2)	F	30	10 million/11d	32 million/8d	21.4 ± 4.77	22.9 ± 2.39	0.30 ± 0.17	1.43 ± 0.45*	18	70	84	84	84
62 yr (case 3)	M	25	12 million/10d	84 million/4d	15.2 ± 0.53	15.8 ± 0.98	0.40 ± 0.03	0.65 ± 0.07*	47	61	78	81	78

^aThree milliliter of bone marrow from three patients (cases 1, 2, and 3) were divided into two T-75 flasks and cultured for several days (primary culture). The numbers indicate the total number of adhering cells obtained from these two flasks after 10 to 11 days (d) culture.

^bThe primary cells were trypsinized and seeded on other T-75 flasks as first passage cells (P1). The numbers indicate the total number of cells in these flasks after 4 to 8 days (d) culture and indicate the proliferation capability of mesenchymal cells from 3 ml of the patient bone marrow used in the present study. The P1 cells were trypsinized and cultured as P2 cells on the ceramic ankle prosthesis for fabrication of the tissue engineered prosthesis as well as in culture dishes for monitoring proliferation and osteoblastic differentiation capability.

^cProliferation capability of the p2 cells cultured with (+) or without (-) Dex in culture dishes as represented in DNA contents.

^dOsteoblastic differentiation capability of p2 cells in culture dishes as represented by ALP activity. Data is presented as mean ± SE (N = 6). Statistical analysis was performed using ANOVA to compare cells cultured with or without Dex (*p < 0.001; **p < 0.01; others, no significance).

^eThe clinical evaluation (maximum score 100) was completed before and 3–24 months (M) after the operation using the tissue engineered prosthesis.

reached confluence after 10 to 11 days (Table 1), when the cells were released from the substratum using 0.05% trypsin, 0.53 mM EDTA. Then 5×10^5 cells of the first passage cells (P1) were put into another T-75 flask and further cultured for several days to expand the number of adherent mesenchymal cells.

The cells were trypsinized, centrifuged, and condensed at the cell density of 5×10^5 cells/ml (second passage cells: P2). Three milliliter of the cell suspension was applied to the ceramic surface (1×10^5 cells/cm²) and incubated overnight. Then 20 ml of the medium was supplemented with 10 mM beta-glycerophosphate disodium salt, pentahydrate, 82 µg/ml L-ascorbic acid phosphate magnesium salt *n*-hydrate, and 100 nM dexamethasone. The ceramic with the cells applied was cultured for 2 weeks, then implanted in the patients or checked for the osteogenic capability (ALP stain and alizarin Red S stain). The P2 cells were also seeded/cultured at a density of 2×10^4 cells/well of a 12-well culture plate in the medium supplemented with/without dexamethasone for assay of cellular activity (Table 1; DNA contents and ALP activity).

2.3. Biochemical assay

We calculated the number of cells after trypsinization using a cell counter (Sysmex, Kobe, Japan). The P2 cells seeded on the ceramic surface and cultured were washed twice with PBS, rinsed with water, and used for ALP and alizarin Red S stain as previously reported [10,11]. The P2 cells cultured in the 12-well plates were washed twice with PBS and scraped off into 0.5 ml of 10 mM Tris-HCl buffer [pH 7.4], 1 mM EDTA, and 0.1 M NaCl. The cells in the buffer were homogenized and sonicated. Then 0.02 ml of the sonicated cell suspension was used for DNA measurements, using salmon sperm DNA as a standard. The DNA measurements were done by fluorescence emission at 458 nm in the presence of 5 µg/0.2 ml of Hoechst 33258. For the measurement of ALP activity, another 0.02 ml of the sonicated cell suspension was centrifuged at 12000 rpm for 1 min, then ALP activity was measured after incubation for 30 min at 37 °C with 0.2 ml of para-nitro phenyl phosphate solution (Zymed, California, USA). ALP activity was represented as µmol of *p*-nitrophenol released per well [10,11]. For analysis of the cell surface antigen, the cells were trypsinized, then incubated with fluorochrome-conjugated antibody on ice for 30 min in the dark, rinsed twice with cold phosphate buffered saline PBS (-) containing 10% Block Ace™ (Dainippon Pharmaceutical Co. Ltd., Osaka, Japan) and then analyzed using a FACSCalibur (Becton-Dickinson, CA, USA) with a minimum of 10,000 events counted after passed through cell strainers (Becton-Dickinson) to remove any cell clumps. The antibodies used were CD13-FITC, CD14-FITC, CD34-FITC, CD45-FITC (CALTAG, CA,

USA); CD29-FITC (Serotec, Oxford, UK); CD90-FITC (Becton-Dickinson, CA, USA); mouse IgG-FITC as isotype controls (Immunotech, Marseille, France).

2.4. Total ankle prosthesis

Alumina (Al₂O₃) ceramic prosthesis was made by Kyocera Co. (Kyoto, Japan) [12]. As seen in Fig. 3a, some portion of the ceramic surface is covered with alumina beads. Thus the surface structure is partly porous, and the cells can easily remain and proliferate.

2.5. Total ankle arthroplasty and clinical evaluation

After resection of the tibia-talus joint portion through an anterior approach (Fig. 1e) [12,13], we inserted the prosthesis. The tibia component was attached with a screw and talus component that was set without screw fixation (Fig. 4b). After the operation, we applied a cast below the knee for 4 weeks and recommended that the patients engage in partial weight bearing starting 2 weeks after the operation and full-weight bearing starting 8 weeks after the operation. Clinical evaluation was undertaken using a clinical ankle score [13,14]. The score had a maximum of 100 points, 60 points for function, and 40 points for perceived pain. A resulting score of 90–100 was considered excellent, 80–89 good, 70–79 fair, and any score less than 70 poor. At the time of the evaluation, the patients also received ordinary anterior-posterior or lateral X-rays of their ankle joints.

3. Results

To obtain adherent cells, we aspirated the patient bone marrow by needle and cultured it in a flask (Fig. 1a). The number of adherent cells grew and reached several millions after 10 to 11 days (Table 1). The cells were collected after trypsinization (first passage: P1) and further cultured in other flasks. After 4 to 8 days, the shape of most cells was fibroblastic (Fig. 1b) and the cells were negative for hematopoietic markers (CD14, 34, 45) but positive for markers present in mesenchymal cells (CD13, 29, 90; Fig. 2). These findings indicate that the adherent fibroblastic cells were mesenchymal types [15]. Thus, we achieved an increase in the number of mesenchymal cells from a small bone marrow fraction.

The cells were trypsinized (second passage: P2), then applied to the ceramic surface (Fig. 1c) and cultured in the medium supplemented with beta-glycerophosphate, vitamin C, and dexamethasone (Dex) for 2 weeks. Some of the cells were also cultured on a 12-well polystyrene plate and another prosthesis to monitor cell proliferation and differentiation capacity. As seen in Table 1, the P2 cells cultured with Dex showed higher ALP activity

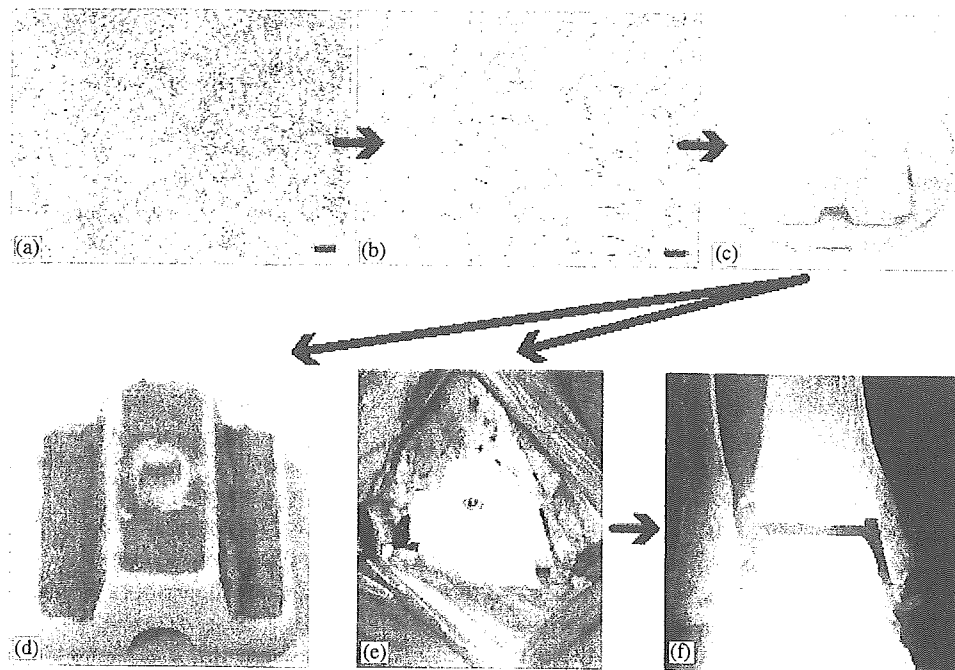


Fig. 1. Approach for fabricating tissue engineered total ankle prostheses. (a) Adhering fibroblastic cells among many red blood cells can be detected several days after primary culture of human bone marrow cells. Bar indicates 100 μm . (b) The number of adhering cells was increased after trypsin treatment and culturing. The figure shows second passage cells (P2) after 3 days of culturing. Almost all cell shapes are fibroblastic. Bar indicates 100 μm . (c) Applying the P2 cells to porous surfaces of alumina ankle prosthesis. (d) To check their osteoblastic differentiation, p2 cells were cultured on an alumina ankle prosthesis for 2 weeks in the presence of Dex; alkaline phosphatase (ALP) stain was performed. Red color indicates high ALP activity. (e) Total joint arthroplasty using another cell-seeded ankle prosthesis without ALP stain. (f) X-ray photo immediately after the operation.

compared with the cells cultured without Dex. The P2 cells cultured with Dex on the prosthesis showed a strong alkaline phosphatase (ALP) stain (Figs. 1d and 3c) and an obvious calcium accumulation evidenced by Alizarin red S stain (Fig. 3d). These data indicate that the surface of the prosthesis was covered with a patient-derived cultured osteoblasts/bone matrix. Thus, we succeeded in fabricating a tissue engineered total ankle prosthesis.

Using the tissue engineered prosthesis, we operated on three patients 62–70 years old having osteoarthritic changes of their ankle joints (Fig. 4a). The follow-up period was 25 to 30 months (Table 1). None of the patients exhibited any obvious inflammation or complications such as infection. We followed the patients' progress with periodic clinical and X-ray examinations. Before the operation, the average clinical score was 26, while at 3, 6, 12, and 24 months after the operation, the scores were 72, 86, 87, and 86, respectively (Table 1). The X-ray findings showed that radiodense areas (indicating bone formation) began to appear around the cell-seeded areas on the prosthesis about 2–3 months after the operation (Fig. 5 2M). Since then, the areas become clearly noticeable (Fig. 5 1Y). The initial radiodense appearance together with a good clinical score proved the establishment of a stable host bone–

prosthesis interface within a few months after the operation. Two years after the operation, the interface was quite durable (Fig. 5 2Y) and showed high clinical scores (Table 1). Therefore, the tissue engineered approach using mesenchymal cells could be used to avoid aseptic loosening of ankle arthroplasty. The stable interface (radiodense areas; indicated by arrows in the dotted areas of Fig. 5) was localized in the porous areas (gray color in the right portion of Fig. 3b) of the implants where the cultured cells were seeded. However, the unseeded areas (white color in Fig. 3b) of the implants did not show bone fixation at any time after the surgery. The findings confirmed the importance of porous architecture and cell seeding (tissue engineering approach) for early bone fixation.

4. Discussion

In the present study, we focused on a total ankle prosthesis composed of alumina (Al_2O_3) ceramic. Alumina ceramics have been reported to show excellent mechanical and good biocompatible properties, however they are bioinert and do not have bone-bonding properties [16–18]. Furthermore, the ankle is a small joint, where a prosthesis is required to tolerate an

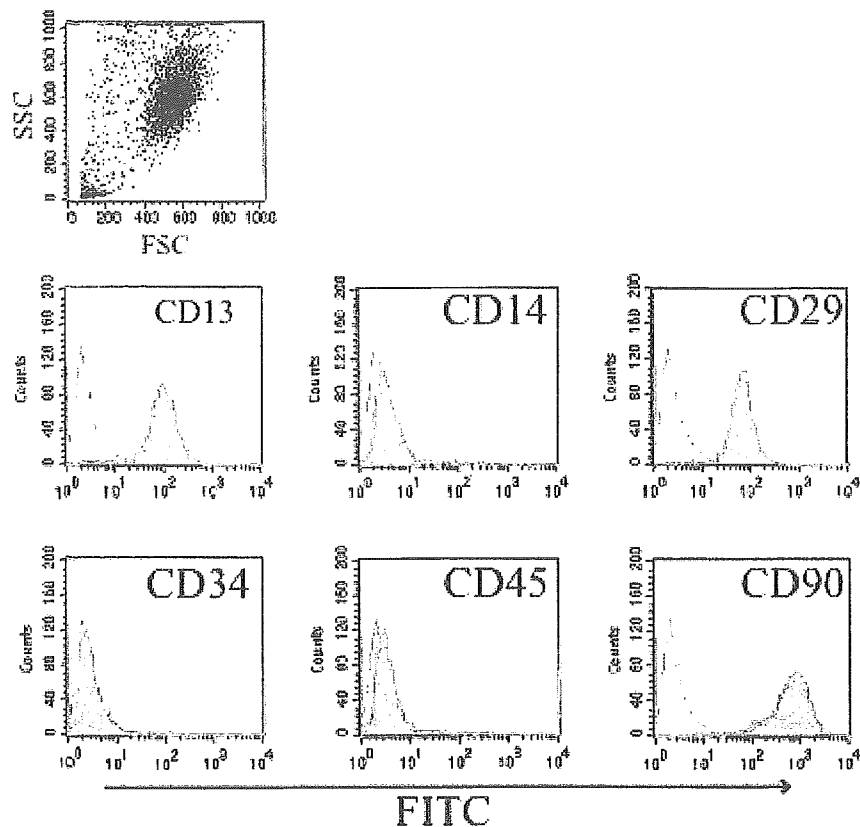


Fig. 2. Comparison of cell surface antigen expression of the P2 cells. Dot plots indicate cell size (forward scatter, FSC) and cell structure (side scatter, SSC). White column indicates peak of negative control; gray column indicates that of each CD expression. Cell surface antigen analysis reveals that CD14, CD34, and CD45 are negative but CD13, CD29, and CD90 are positive. These findings indicate that the P2 cells are mesenchymal types.

excessive load per unit area. Therefore, the rate of loosening and subsidence of an alumina ankle prosthesis is very high; we have experienced a rate of about 50% over a 5-year period [12]. One possible solution in overcoming this problem is to coat the ceramic surface with hydroxyapatite (HA) because this coating on a large joint prosthesis is thought to provide safe and stable fixation [19,20]. However, a flat alumina surface coated with HA does not have a stable interface and, thus, its porous areas must be coated with HA. Coating the porous areas is difficult and besides, inorganic materials including HA usually do not exhibit biological functions such as new bone-forming capability.

Concerning bone-forming capability, fresh bone marrow contains mesenchymal cells, which can exhibit osteogenic differentiation. Therefore, an ankle prosthesis coated with HA and supplemented with the patient's fresh marrow cells can be expected to show good clinical results. In fact, we have used this sort of composite ankle prosthesis and achieved excellent/good results in 86% of the patients [12]. However, because of the extremely small number of MSCs in fresh bone marrow, the present paper reports on our use of a tissue

engineering approach to increase the number of MSCs followed by osteogenic differentiation together with bone matrix formation prior to joint arthroplasty (Fig. 3d). This approach includes a process of culturing mesenchymal cells on a bioinert alumina ceramic surface and, thus, it requires the provision of suitability of a ceramic surface for culturing. In this regard, we reported that the capability of a ceramic surface to support human mesenchymal cell proliferation/differentiation was comparable to that of a plasma treated polystyrene tissue culture dish surface [21], which is recognized as the gold standard substratum for cell culture [22].

As seen in Fig. 3C and D, the differentiation of MSCs on an alumina ankle prosthesis resulted in bone matrix formation as well as the appearance of active osteoblasts inside the pore regions of the ceramics. The matrix is composed of a mineral component such as HA crystal and an organic component that is largely collagen fibers together with various growth factors/cytokines [10–11,23]. Therefore, we have succeeded in fabricating a tissue engineered total ankle prosthesis, which can be expected to exhibit successful bone–prosthesis fixation [6]. As seen in Fig. 5, present clinical cases showed a

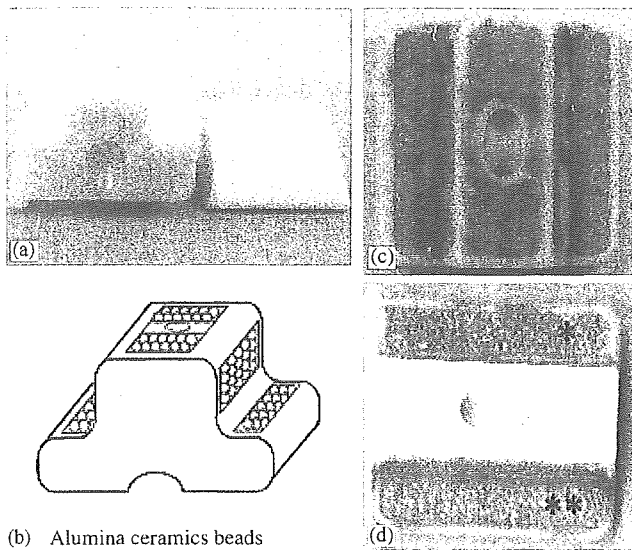


Fig. 3. Tissue engineered total ankle prosthesis. (a) The prosthesis consists of tibia and talus (dome shape) alumina components and soft wear-resistant white polyethylene, which is attached to the bottom of the tibia component. (b) Schematic presentation of tibia alumina component. Some surface areas consist of clusters of ceramic beads (represented in gray). Thus, the surface is porous, and the cells can be easily applied. (c) Cultured patient P2 cells were seeded on the surface of tibia ceramic component and cultured with Dex for 2 weeks. ALP staining was then performed on the entire surface (see also Fig. 1d). (d) To confirm bone matrix formation (mineralization), ALP staining (*) and Alizarin red S (**) staining were performed independently on the surface side areas. Red indicates ALP and Alizarin red S positive areas.

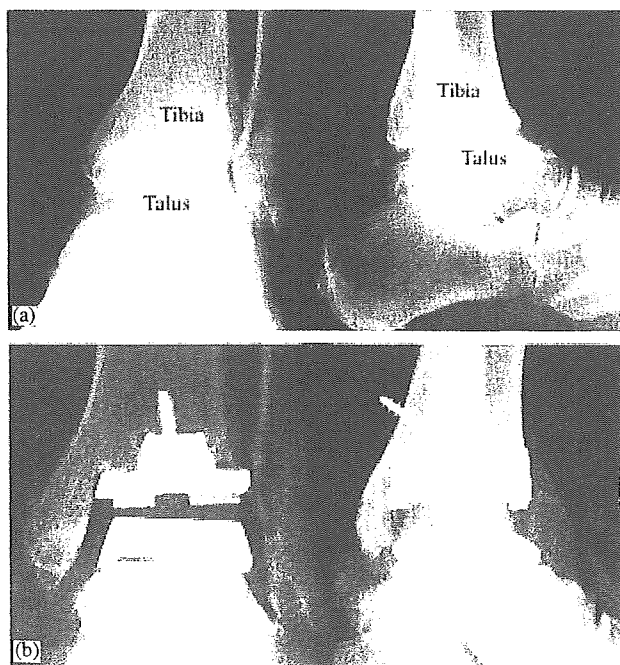


Fig. 4. (a) X-ray photograph of ankle joint (case 3) before the operation. Left: anterior–posterior (AP) view. Right: lateral view. The joint space between the tibia and talus is barely recognizable, indicating severe osteoarthritic change. (b) X-ray photograph of case 3 immediately after operation using the tissue engineered ceramic total ankle prosthesis. Left: AP. Right: Lateral view.

prompt radiodense appearance around the cell-seeded areas on the prosthesis indicating stable fixation. In our basic experiments, we reported that the tissue engineered material (bone matrix/osteoblast construct) shows immediate new bone-forming capability after *in vivo* implantation. In addition, the new bone can bond to a prefabricated bone matrix surface [24]. We also found that tissue engineered alumina ceramics exhibited higher mechanical interface between the ceramic surface and host bone than did untreated ceramics in a rabbit model (Thoma et al., manuscript in preparation). Therefore, our basic as well as clinical experience demonstrated that the osteoblast/bone matrix formed on alumina ceramics can show further *in vivo* osteogenic function resulting in a stable interface between the tissue engineered ceramic surface and the host bone. Because the length of the present follow-up period is only about two years, a much longer period is required to confirm a stable interface.

Fabrication of a tissue engineered total ankle prosthesis requires the use of the patient's marrow that has osteogenic function [5–8,24–26]. The amount of marrow required is very small (only 3 ml) and due to the minimum invasion (needle aspiration), none of the patients complained of severe pain or required hospitalization until the actual joint surgery. Furthermore, the use of an engineered prosthesis consisting of autologous cells did not exhibit immunological reactions and did not cause inflammation around the implanted areas. Although this paper describes a novel method of using patient mesenchymal cells to prevent loosening in total ankle arthroplasty, the method can be applied on any type of arthroplasty. In addition, the mesenchymal cells can be cultured/differentiated into osteoblasts on many other biomaterials including metals and polymers [11,27]. Therefore, this tissue engineering approach may be used for a variety of clinical applications in the fields of orthopedic, craniomaxillofacial, and plastic surgery.

5. Conclusion

Although the number of patients analyzed in the present paper was very small and control studies such as simple hydroxyapatite coating on ceramic ankle prostheses have not been done, all of the three cases showed high clinical scores with stable host bone–prosthesis interface. Therefore, the present tissue engineered method using mesenchymal cells derived from patient bone marrow can be expected to show early bone fixation around the cell-seeded areas on alumina ceramics. Further substantial work is needed to prove the effectiveness of the current approach using tissue engineered ankle prostheses that are not subject to loosening.

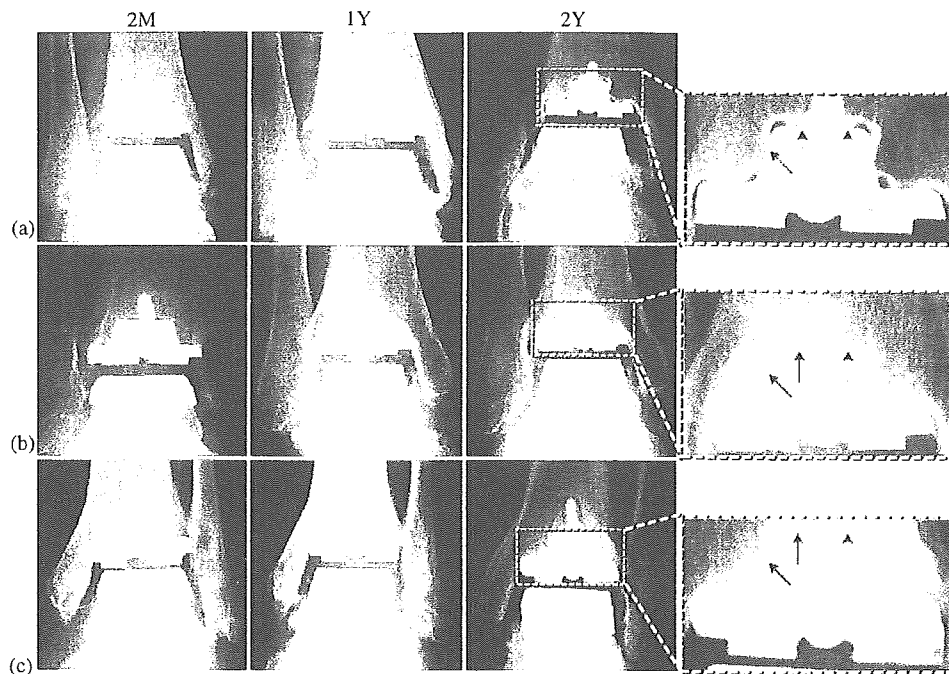


Fig. 5. X-ray photographs (AP views) of three cases after the operations. (a–c) are photographs of case 1, case 2, and case 3, respectively. Photographs are 8 to 10 weeks (2M), about one (1Y), and 2 years (2Y) after the operation. Implanted tibial component regions at 2 years are magnified and represented in the right-hand photographs. In the left-hand photographs (2M), early bone adaptation by newly formed bone can be seen. A stable bone/implant interface was clearly detected at both 1 and 2 years after the operation. Tight bone/implant fixation can be seen on the porous areas of the implants seeded with mesenchymal cells (arrows). However, fixation is barely seen on the smooth surface areas of the implants where the cells could not grow well.

References

- [1] Kitaoka HB, Patzer GL. Clinical results of the Mayo total ankle arthroplasty. *J Bone Joint Surg Am* 1996;78(11):1658–64.
- [2] Kofoed H, Sorensen TS. Ankle arthroplasty for rheumatoid arthritis and osteoarthritis: prospective long-term study of cemented replacements. *J Bone Joint Surg Br* 1998;80(2):328–32.
- [3] Michelson JD, Schmidt GR, Mizel MS. Kinematics of a total arthroplasty of the ankle: comparison to normal ankle motion. *Foot Ankle Int* 2000;21(4):278–84.
- [4] Caplan AI. Mesenchymal stem cells. *J Orthop Res* 1991;9(5):641–50.
- [5] Gao J, Caplan AI. Mesenchymal stem cells and tissue engineering for orthopaedic surgery. *Chir Organi Mov* 2003;88(3):305–16.
- [6] Ohgushi H, Caplan AI. Stem cell technology and bioceramics: from cell to gene engineering. *J Biomed Mater Res* 1999;48(6):913–27.
- [7] Petite H, Viateau V, Bensaid W, Meunier A, de Pollak C, Bourguignon M, et al. Tissue-engineered bone regeneration. *Nat Biotechnol* 2000;18(9):959–63.
- [8] Mendes SC, Tibbe JM, Veenhof M, Bakker K, Both S, Platenburg PP, Oner FC, De Bruijn JD, Van Blitterswijk CA. Bone tissue-engineered implants using human bone marrow stromal cells: effect of culture conditions and donor age. *Tissue Eng* 2002;8(6):911–20.
- [9] Kruyt MC, van Gaalen SM, Oner FC, Verbout AJ, de Bruijn JD, Dhert WJ. Bone tissue engineering and spinal fusion: the potential of hybrid constructs by combining osteoprogenitor cells and scaffolds. *Biomaterials* 2004;25(9):1463–73.
- [10] Ohgushi H, Dohi Y, Katuda T, Tamai S, Tabata S, Suwa Y. In vitro bone formation by rat marrow cell culture. *J Biomed Mater Res* 1996;32(3):333–40.
- [11] Ohgushi H, Dohi Y, Yoshikawa T, Tamai S, Tabata S, Okunaga K, et al. Osteogenic differentiation of cultured marrow stromal stem cells on the surface of bioactive glass ceramics. *J Biomed Mater Res* 1996;32(3):341–8.
- [12] Takakura Y, Tanaka Y, Kumai T, Sugimoto K, Ohgushi H. Ankle arthroplasty using three generations of metal and ceramic prostheses. *Clin Orthop* 2004;424:130–6.
- [13] Takakura Y, Tanaka Y, Sugimoto K, Tamai S, Masuhara K. Ankle arthroplasty. A comparative study of cemented metal and uncemented ceramic prostheses. *Clin Orthop* 1990;252:209–16.
- [14] Takakura Y, Tanaka Y, Sugimoto K, Akiyama K, Tamai S. Long-term results of arthrodesis for osteoarthritis of the ankle. *Clin Orthop* 1999;361:178–85.
- [15] Campagnoli C, Roberts IA, Kumar S, Bennett PR, Bellantuono I, Fisk NM. Identification of mesenchymal stem/progenitor cells in human first-trimester fetal blood, liver, and bone marrow. *Blood* 2001;98(8):2396–402.
- [16] Klawitter J, Hulbert S. Application of porous ceramics for the attachment of load bearing internal orthopedic application. *J Biomed Mater Res* 1971;2:161–229.
- [17] Predecki P, Auslaender BA, Stephan JE, Mooney VL, Stanitski C. Attachment of bone to threaded implants by ingrowth and mechanical interlocking. *J Biomed Mater Res* 1972;6(5):401–12.
- [18] Takaoka T, Okumura M, Ohgushi H, Inoue K, Takakura Y, Tamai S. Histological and biochemical evaluation of osteogenic response in porous hydroxyapatite coated alumina ceramics. *Biomaterials* 1996;17(15):1499–505.

- [19] Hamadouche M, Witvoet J, Porcher R, Meunier A, Sedel L, Nizard R. Hydroxyapatite-coated versus grit-blasted femoral stems. a prospective, randomised study using EBRA-FCA. *J Bone Joint Surg Br* 2001;83(7):979–87.
- [20] Overgaard S, Lind M, Glerup H, Grundvig S, Bunger C, Soballe K. Hydroxyapatite and fluorapatite coatings for fixation of weight loaded implants. *Clin Orthop* 1997;336: 286–96.
- [21] Kitamura S, Ohgushi H, Hirose M, Funaoka H, Takakura Y, Ito H. Osteogenic differentiation of human bone marrow-derived mesenchymal cells cultured on alumina ceramics. *Artif Organs* 2004;28(1):72–82.
- [22] Kotobuki N, Ioku K, Kawagoe D, Fujimori H, Goto S, Ohgushi H. Observation of osteogenic differentiation cascade of living mesenchymal stem cells on transparent hydroxyapatite ceramics. *Biomaterials* 2005;26(7):779–85.
- [23] Maniopoulos C, Sodek J, Melcher AH. Bone formation in vitro by stromal cells obtained from bone marrow of young adult rats. *Cell Tissue Res* 1988;254(2):317–30.
- [24] Yoshikawa T, Ohgushi H, Tamai S. Immediate bone forming capability of prefabricated osteogenic hydroxyapatite. *J Biomed Mater Res* 1996;32(3):481–92.
- [25] Ohgushi H, Okumura M. Osteogenic capacity of rat and human marrow cells in porous ceramics. Experiments in athymic (nude) mice. *Acta Orthop Scand* 1990;61(5):431–4.
- [26] Bruder SP, Jaiswal N, Haynesworth SE. Growth kinetics, self-renewal, and the osteogenic potential of purified human mesenchymal stem cells during extensive subcultivation and following cryopreservation. *J Cell Biochem* 1997;64(2):278–94.
- [27] Hasegawa Y, Ohgushi H, Ishimura M, Habata T, Tamai S, Tomita N, et al. Marrow cell culture on poly L-lactic acid fabrics. *Clin Orthop* 1999;358:235–43.

Viability and Osteogenic Potential of Cryopreserved Human Bone Marrow-Derived Mesenchymal Cells

NORIKO KOTOBUKI, M.Sc.,¹ MOTOHIRO HIROSE, Ph.D.,¹ HIROKO MACHIDA, M.Sc.,¹
YOUICHI KATOU, B.Sc.,¹ KAORI MURAKI, B.Sc.,¹ YOSHINORI TAKAKURA, M.D.,²
and HAJIME OHGUSHI, M.D.¹

ABSTRACT

Human bone marrow-derived mesenchymal cells contain mesenchymal stem cells (MSCs), which are well known for their osteo/chondrogenic potential and can be used for bone reconstruction. This article reports the viability of cryopreserved human mesenchymal cells and a comparison of the osteogenic potential between noncryopreserved and cryopreserved human mesenchymal cells with MSC-like characteristics, derived from the bone marrow of 28 subjects. The viability of cryopreserved mesenchymal cells was approximately 90% regardless of the storage term (0.3 to 37 months). It is clear by fluorescence-activated cell sorter analysis that the cell surface antigens of both noncryopreserved and cryopreserved mesenchymal cells were negative for hematopoietic cell markers such as CD14, CD34, CD45, and HLA-DR but positive for mesenchymal characteristics such as CD29 and CD105. To monitor the osteogenic potential of the cells, such as alkaline phosphatase (ALP) activity and *in vitro* mineralization, a subculture was conducted in the presence of dexamethasone, ascorbic acid, and glycerophosphate. No difference in osteogenic potential was found between cells with or without cryopreservation treatment. In addition, cells undergoing long-term cryopreservation (about 3 years) maintained high osteogenic potential. In conclusion, cryopreserved as well as noncryopreserved human mesenchymal cells could be applied for bone regeneration in orthopedics.

INTRODUCTION

MESENCHYMAL STEM CELLS (MSCs) are multipotent cells and can be induced *in vitro* and *in vivo* to differentiate into various functional cell types of mesodermal tissues including bone, cartilage, tendon, fat, and bone marrow stroma.¹⁻³ Many researchers, including us, have previously reported that primary cultures of mesenchymal cells derived from bone marrow could differentiate into osteoblasts by treatment with dexamethasone (Dex). The osteoblasts formed extracellular bone matri-

ces with abundant minerals on ceramic surfaces.⁴⁻⁶ On the basis of these results, it has been proposed that autologous mesenchymal cells be used for the treatment of bone/joint diseases.⁷ The mesenchymal cells can differentiate into osteoblasts not only on tissue culture polystyrene (TCPS) dishes but also on the surfaces of biomaterials, such as bioactive calcium phosphate ceramics and bioinert alumina ceramics.⁸ "Regenerative cultured bone tissue," which is a hybrid of culture-differentiated osteoblasts/bone matrix on biomaterials, has already been implanted into patients.⁹

¹Research Institute for Cell Engineering (RICE), National Institute of Advanced Industrial Science and Technology (AIST), Amagasaki, Hyogo, Japan.

²Department of Orthopedic Surgery, Nara Medical University, Kashihara, Nara, Japan.

Studies have also demonstrated the possibility that MSCs can differentiate into other types of tissue-specific cells such as cardiac myoblasts,¹⁰ vascular endothelial cells,^{11,12} hepatocytes,¹³ and neural cells.¹⁴ These results indicate the usefulness of multipotential MSCs for tissue-engineering purposes in regenerative medicine.^{15,16} Bone marrow cells have been utilized as a source of MSCs; however, the number of MSCs to be culture-expanded from fresh bone marrow in a short time is limited and the MSCs cannot survive for long periods under culture conditions. Because MSCs are difficult to isolate from bone marrow, because of the paucity of specific markers, we have used whole adherent cells (mesenchymal cells) from bone marrows that showed high osteogenic potential.

As the technology to preserve cultured cells by freezing methods has progressed,^{17,18} cryopreserved cells have been expected to become cell sources for the fabrication of regenerative tissues and to have potentially important implications for clinical applications in regenerative medicine. This is especially significant because of the limited supply of mesenchymal cells. Therefore, if long-term cryopreserved mesenchymal cells still retain a high level of viability and ability to differentiate into tissue-specific cells, they will be useful as a cell source to regenerative medicine, especially autologous usage to avoid transplantation immunity, not only for bone but also other tissue reconstruction therapy.

We have previously reported that cryopreserved human mesenchymal cells after thawing had more than 90% viability and differentiated into osteoblasts in the presence of Dex.¹⁹ However, only three cases were analyzed and we did not analyze the entire number of cryopreserved cells, only the adherent cells. In this study, we report direct evidence of the viability and osteogenic potential of cryopreserved mesenchymal cells, from 28 donors, which were stored for 0.3 to 37 months. We also compared cell morphology, expression of cell surface antigens, and osteogenic activities between cryopreserved and noncryopreserved mesenchymal cells derived from fresh bone marrow of the same donors.

MATERIALS AND METHODS

Cell preparation and culture method

In accordance with the Ethics Committee at the Tissue Engineering Research Center (Amagasaki, Japan), we obtained informed consent from the bone marrow donors. The age, gender, and results of biological assays of each donor are listed in Table 1. Three milliliters of bone marrow was captured in a 13-mL tube (Assist, Tokyo, Japan) containing the same volume of heparinized (10 U/mL) phosphate-buffered saline (PBS; Invitrogen, Carlsbad, CA). The mixture of bone marrow and heparinized PBS

was centrifuged at $140 \times g$ for 10 min at 4°C and the supernatant of plasma with the fat layer was discarded. The residue (buffy coat together with the red blood cell layer) was put into 75-cm² flasks (BD Biosciences Discovery Labware, Bedford, MA) with basal medium comprising Eagle's minimal essential medium α (α -MEM; Invitrogen) containing 15% fetal bovine serum (FBS; JRH Biosciences, Lenexa, KS) and antibiotics, and then cultured in a humidified atmosphere of 95% air with 5% CO₂ at 37°C .²⁰

At subconfluency, the cell density is about $2.5\text{--}6.5 \times 10^4$ cells/cm²; the mesenchymal cells are detached from the flasks with 0.05% trypsin–0.53 mM EDTA (Invitrogen), concentrated at a density of 5×10^5 cells/mL, and suspended in Cell Banker storage solution (Juji Field, Tokyo, Japan), a ready-to-use storage solution containing dimethyl sulfoxide (DMSO) and fetal bovine serum. As a simplified process of program freezing, mesenchymal cells in the storage solution were stored sequentially at 4°C for 10 min, -30°C for 1 h, and -80°C for 2–3 days. Finally, mesenchymal cells were stored at -152°C for long-term cryopreservation. Noncryopreserved mesenchymal cells from 15 samples (Table 1, nos. 12, 13, and 16–28) and cryopreserved mesenchymal cells from 26 samples (Table 1, nos. 1–6 and 9–28) were seeded on a 12-well plate at a cell density of 1×10^4 /cm² and cultured under osteogenic conditions for 2 weeks. The culture medium was changed three times per week. The osteogenic medium contained 10 mM β -glycerophosphate disodium salt (β -GP; Merck, Darmstadt, Germany), 0.07 mM L-ascorbic acid 2-phosphate magnesium salt n-hydrate (Sigma-Aldrich, St. Louis, MO), and 0.1 μM Dex (Sigma-Aldrich) in the basal medium. In addition, calcitonin ($1 \mu\text{g}/\text{mL}$; Dojindo Laboratories, Kumamoto, Japan) was included in the medium for one of the osteogenic assays, quantitative analysis of calcium contents. As a negative control, cells were cultured in basal medium containing only 10 mM β -GP.

FACS analysis

Cells noncryopreserved before subculture and cells cryopreserved immediately after thawing were incubated with each fluorescein isothiocyanate (FITC)-conjugated anti-cluster of differentiation (CD) antibody on ice for 30 min in the dark. After the wash step, the cells were loaded in a FACSCalibur flow cytometer (BD Biosciences Immunocytometry Systems, San Jose, CA) with a minimum of 10,000 events counted. The antibodies used in this experiment were to CD14, CD34, CD45 (Caltag Laboratories, Burlington, CA), CD29, CD105, and human leukocyte antigen region DR (HLA-DR) (Serotec, Oxford, UK). Mouse immunoglobulin G (IgG) (Beckman Coulter, Fullerton, CA) was used as an isotype control. The fluorescence intensity of each antibody was compared

TABLE 1. DONOR INFORMATION AND VIABILITY AND OSTEOGENIC ACTIVITIES OF NONCRYOPRESERVED AND CRYOPRESERVED HUMAN MESENCHYMAL CELLS^a

ID	Age (years)	Sex (F/M)	Noncryopreserved cells				Cell viability (%)	Storage period (months)	Cryopreserved cells			
			ALP/DNA ($\mu\text{mol}/\mu\text{g}$)		Calcein (FI/area)				ALP/DNA ($\mu\text{mol}/\mu\text{g}$)		Calcein (FI/area)	
			Dex (+)	Dex (-)	Dex (+)	Dex (-)			Dex (+)	Dex (-)	Dex (+)	Dex (-)
1	71	M					81.2	33.3	2.72	0.37	2,909	286
2	27	M					92.8	33.3	0.65	0.11	595	128
3	65	F					87.8	33.6	0.6	0.17	3,057	216
4	66	F					82.9	33	0.66	0.34	3,618	306
5	55	F					89.3	37.3	0.55	0.21	1,613	173
6	77	F					89.3	37	0.53	0.17	5,319	287
7	62	F					99	36				
8	55	F					100	23.6				
9	66	F					83	15	0.166	0.086	3,288	1,747
10	70	F					94.6	15	0.194	0.044	1,980	426
11	61	M					100	12	0.222	0.023	157	112
12	62	M	0.185	0.086	4,190	214		6	0.16	0.05	5,436	132
13	54	F	0.358	0.106	5,900	2,620		7	0.13	0.1	3,117	147
14	71	M						0.6	0.03	0.01	1,971	125
15	70	F					91.1	6	0.851	0.064	4,027	2,131
16	69	F	0.119	0.091	9,017	99		0.3	0.09	0.02	812	120
17	58	M	0.172	0.081	11,994	88		1.3	0.2	0.08	6,526	156
18	25	M	0.307	0.042	6,740	53		1.3	0.34	0.06	3,591	171
19	75	F	0.278	0.086	10,168	42		1.3	0.36	0.14	3,263	201
20	42	M	0.471	0.124	3,027	68	71.9	5.3	0.322	0.061	5,267	131
21	42	M	0.573	0.001	4,746	4,836	84.9	5.5	0.24	0.178	2,741	889
22	72	F	0.27	0.085	3,156	33	92.2	5.6	0.289	0.125	2,149	355
23	14	M	0.322	0.072	2,447	26	91.4	5	0.453	0.047	1,243	33
24	77	M	0.21	0.124	3,317	114	96.4	4.3	0.472	0.405	2,501	189
25	8	M	0.417	0.312	4,918	1,140	88	5	0.63	0.058	2,800	97
26	83	M	0.405	0.14	5,528	216	98.3	4.3	0.55	0.064	4,208	107
27	70	F	0.33	0.077	9,719	231	95.6	3.6	0.912	0.216	2,206	143
28	29	M	0.687	0.113	5,020	301	85.4	3	0.815	0.078	4,096	134

^aIndependent donors are listed by ID numbers. Mesenchymal cells were cultured with or without Dex for 2 weeks. ALP activity was measured by enzymatic reaction using pNPP. Calcium deposition was measured by detecting the fluorescence intensity (FI) of calcein deposited in the extracellular matrix of the cell culture. All data represent the mean of six independent experiments. The viability of stored (cryopreserved) cells immediately after thawing was measured with a NucleoCounter. Blanks, no data.

with that of the isotype control and represented as a histogram.

Cell viability assay

The viability of cryopreserved cells from 21 samples (Table 1, nos. 1–11, 15, and 20–28) was analyzed with a NucleoCounter (ChemoMetec, Allerød, Denmark). Because the detection principle is based on staining nuclei with a dye, it is evident that in order to stain the nuclei they must be permeable to the dye. The dye cannot penetrate a viable cell and thus it is necessary to lyse the cell membrane before staining. Nonviable cells, on the other hand, are permeable and can therefore be stained with the nuclear

dye. Using this property of nonviable cells and combining results obtained from samples that have not been lysed (nonviable cell count) and the result obtain by lysing cells (a total cell count), it becomes possible to use the NucleoCounter to estimate the viability of a cell sample.

Immediately after thawing, cryopreserved cells were diluted by a factor of 10 with culture medium. Cell suspensions were centrifuged at $400 \times g$ for 5 min and resuspended with 5 mL of culture medium. Two hundred microliters of each cell sample was analyzed on the NucleoCounter with cartridges before and after treatment with a lysis buffer, giving an estimate of nonviable and total cells, respectively. The manual counting method was based on the trypan blue exclusion procedure.